# THE X-RAY BACKGROUND AND THE DEEP X-RAY SURVEYS

R. Gilli[1]

[1]*Istituto Nazionale di Astrofisica (INAF), Osservatorio Astrofisico di Arcetri, Largo E. Fermi 5, 50125 Firenze, Italy*

## ABSTRACT

The deep X-ray surveys performed by the two major X-ray observatories on flight, Chandra and XMM, are being resolving the bulk of the cosmic X-ray background (XRB) in the 2–10 keV energy band, where the sky flux is dominated by extragalactic emission. Although the actual fraction depends on the absolute sky flux, which is measured with an uncertainty of $\sim 40\%$, most of the XRB is already resolved. Optical identifications of the X-ray sources in the deep surveys are being showing that these are mainly AGN, most of which being obscured as predicted by population synthesis models. However, first results indicate that the redshift distribution of the sources making the XRB seems to peak at much lower redshift than predicted by the models. In this article I will briefly review and discuss the measurements of the XRB spectrum and the AGN synthesis models of the XRB. Then, I will introduce the Chandra and XMM deep X-ray surveys, mainly focusing on the Chandra Deep Field North and South. Finally, the properties of the X-ray sources populating the deep surveys will be described and compared with the predictions of the most recent synthesis models.

## INTRODUCTION

The origin of the X-ray background in the 2-10 keV energy range has been finally understood. The extremely deep surveys by Chandra in the Deep Field South (Giacconi et al. 2002; Rosati et al. 2002) and Deep Field North (Brandt et al. 2001; Barger et al. 2002) have shown that most, if not all, the XRB emission in that energy range has been resolved into single sources. In particular, the optical and X-ray properties of the sources in the deep fields are showing that the main contribution is provided by a population of obscured AGN. This confirms the main prediction of population synthesis models (e.g. Setti & Woltjer 1989; Comastri et al. 1995; Fabian et al. 1999; Gilli, Salvati & Hasinger 2001), which explain the XRB spectrum in the $\sim 1-100$ keV band as the emission integrated over cosmic time of unobscured and obscured AGN, the latter being more numerous by a factor of $\sim 4-10$. Once the origin of the 2-10 keV XRB is finally explained, the results from the deep surveys, combined with synthesis models, should put tighter constraints on the cosmological properties of the sources making the XRB, like their X-ray luminosity function and evolution (especially those of obscured AGN, which are still completely unknown), as well as their average obscuration as a function of redshift and luminosity.

## THE COSMIC X-RAY BACKGROUND MEASUREMENTS

At present, in the 10–100 keV range, where the bulk of the XRB energy resides, the only available measurements are those performed in the late 1970s by HEAO-1 (Marshall et al. 1980; Gruber 1992). The data showed that the XRB spectrum has a characteristic "bell" shape peaking at $\sim 30-40$ keV, which, at lower energies, can be approximated by a power-law with photon index $\Gamma = 1.4$. A recent reanalysis of HEAO-1 data by Gruber et al. (1999) confirmed those earlier results, but also showed that the calibration uncertainties among HEAO-1 detectors are of the order of 10% in the overlapping energy bands (Fig. 1).

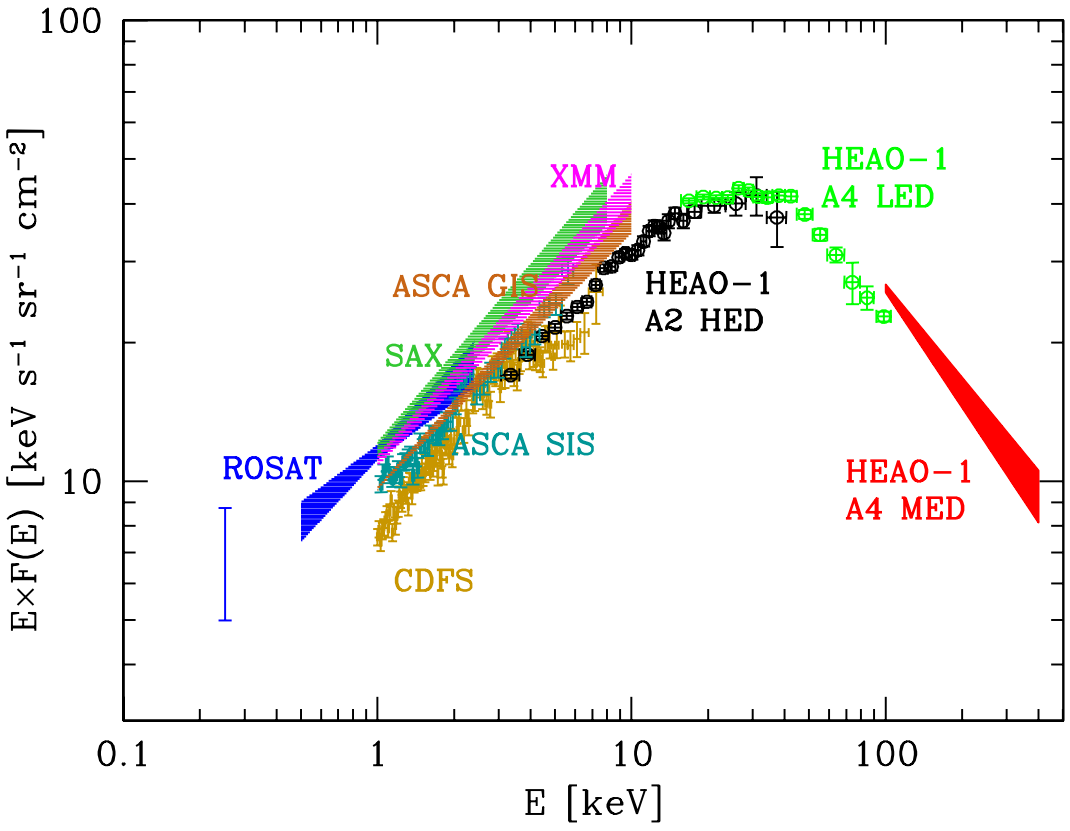


Fig. 1. The extragalactic X-ray background spectrum from 0.2 to 400 keV. Different colors correspond to measurements by different missions/instruments as labeled. The reference list for the shown data is the following: ROSAT 0.25 keV (Warwick & Roberts 1998); ROSAT 0.5-2.4 keV (Georgantopoulos et al. 1996); HEAO-1 A2 HED + A4 LED (Gruber 1992; Gruber et al. 1999); HEAO-1 A4 MED (Kinzer et al. 1997); SAX (Vecchi et al. 1999); ASCA SIS (Gendreau et al. 1995); ASCA GIS (Kushino et al. 2002); XMM (Lumb et al. 2002); CDFS (Tozzi et al. 2001a).

The situation is more complicated at lower energies where a number of measurements have been obtained. While the spectral slope of the 2–10 keV XRB has always been found to have small variations around $\Gamma = 1.4$, there are significant discrepancies in the spectral normalization. From the highest (11.5 keV $s^{-1}$ $sr^{-1}$ $cm^{-2}$ $keV^{-1}$ ; SAX, Vecchi et al. 1999) to the lowest measured value (8 keV $s^{-1}$ $sr^{-1}$ $cm^{-2}$ $keV^{-1}$ ; HEAO-1, Marshall et al. 1980) the variation is of the order of $\sim 40\%$. The most recent measuments have been obtained by Kushino et al. (2002) from a combination of 91 ASCA GIS fields, with a total sky coverage of 50 $deg^2$, and by Lumb et al. (2002) from a combination of 8 XMM pointings covering 6.5 $deg^2$ in total. The XRB spectral slope is found to be $\Gamma = 1.412 \pm 0.032$ and $\Gamma = 1.42 \pm 0.03$ in the ASCA and XMM data, respectively (errors are at 90% confidence level), again very close to $\Gamma = 1.4$. The power-law normalizations ($9.66 \pm 0.07$ and $11.1 \pm 0.32$ keV $s^{-1}$ $sr^{-1}$ $cm^{-2}$ $keV^{-1}$ for the ASCA and XMM data, respectively, including the resolved bright sources) are within the range already spanned by previous missions, but do not suggest that the measurements of the XRB intensity are converging to a well constrained value. Interestingly, all the measurements of the 2-10 keV XRB intensity since HEAO-1 are higher than the HEAO-1 value.

## AGN POPULATION SYNTHESIS MODELS

In 1989, when the resolved XRB fraction was just a few percent, Setti & Woltjer (1989) proposed that the flat slope of the 2–10 keV XRB was due to a population of obscured AGN in addition to the bright unobscured AGN with steep spectra observed at that time. Since then, a number of models have been worked out and refined constantly (Madau, Ghisellini & Fabian 1994; Comastri et al. 1995; Pompilio, La

Franca & Matt 1999; Wilman & Fabian 1999). With the increasing sensitivity of recent X-ray surveys, the population of obscured AGN emerged (see e.g. Mushotzky et al. 2000), and the main prediction of the AGN synthesis models was then confirmed. However, given the large number of uncertain parameters involved, it is crucial to check synthesis models against the largest number of observational constraints. The main uncertainties are related to unobscured AGN. While the X-ray luminosity function (XLF) and evolution of unobscured AGN are rather well known (e.g. Miyaji, Hasinger & Schmidt 2000), nothing is known about obscured AGN. Comastri et al. (1995) showed that, assuming for the obscured AGN a distribution of absorbing columns and the same evolution and XLF (upscaled by a factor of a few) of unobscured ones, it was possible to fit the full XRB spectrum in the $\sim 1-100$ keV band, as well as the integral counts (logN-logS relation) in the 0.5-2 keV and 2-10 keV energy bands. Also, the redshift distribution of AGN detected in ROSAT and HEAO-1 samples (at limiting fluxes of $f_{0.5-2} \sim 10^{-14}$ erg cm$^{-2}$ s$^{-1}$ and $f_{2-10} \sim 3\,10^{-11}$ erg cm$^{-2}$ s$^{-1}$ , respectively) were in good agreement with the model expectations. Later, more constraints became available. The local ratio between obscured and unobscured AGN (in the Seyfert luminosity regime) was found to be $\sim 4$ (Maiolino & Rieke 1995), and the column density distribution of local Seyfert 2s was determined (Risaliti et al. 1999). Using these new constraints it was shown (Gilli, Risaliti & Salvati 1999) that, if the column density distribution in obscured AGN is the same at all redshifts and luminosities, then additional obscured sources at moderate/high redshifts are required to match the XRB constraints. Gilli, Salvati & Hasinger (2001, hereafter GSH01) proposed that obscured sources evolve slightly faster than unobscured ones. In particular they favored a model (model B) where the ratio between obscured and unobscured AGN increases from 4 at $z = 0$ to 10 at $z = 1.3$, where both populations stop evolving. This model was able to reproduce the broad set of observational constraints used by Comastri et al., furthermore extending the agreement to lower fluxes. In particular, the redshift distribution of soft X-ray selected AGN in the ROSAT Ultra Deep Survey (UDS, Lehmann et al. 2001) at a limiting flux of $f_{0.5-2} \sim 10^{-15}$ erg cm$^{-2}$ s$^{-1}$ was nicely reproduced, as well as that of hard X-ray selected AGN in the ASCA Large Sky Survey (Akiyama et al. 2000) at a limiting flux of $f_{2-10} \sim 10^{-13}$ erg cm$^{-2}$ s$^{-1}$ . Moreover, AGN synthesis models showed that, while the XRB spectrum can be simply fitted with a population of Seyfert 2 galaxies in addition to unobscured AGN, the ASCA and BeppoSAX source counts in the hard band are matched only by assuming a population of luminous obscured AGN, the so-called QSO2s (GSH01; Comastri et al. 2001). It is here noted that the main contribution to the source counts is expected to be produced by QSO2s with column densities in the range $\log N_H = 22-23$, while the contribution of Compton thick QSO2s is expected to be negligible.

## THE DEEP X-RAY SURVEYS

A number of deep ($\sim$ Ms) and moderately deep ($\sim$ 200 ks) X-ray surveys are being conducted in different sky fields with Chandra and XMM.

The Chandra Deep Field North (CDFN, Brandt et al. 2001) and the Chandra Deep Field South (CDFS, Giacconi et al. 2002; Rosati et al. 2002) have been observed with the ACIS-I array for 2 Ms and 1 Ms respectively, and represent the two deepest X-ray surveys to date. In the 2 Ms CDFN the achieved sensitivity limit is $\sim 1.5\,10^{-17}$ erg cm$^{-2}$ s$^{-1}$ in the soft band and $\sim 1.0\,10^{-16}$ erg cm$^{-2}$ s$^{-1}$ in the hard band (Alexander et al. 2002). In the CDFS the sensitivity limits of $f_{0.5-2} \sim 5.5\ 10^{-17}$ erg cm$^{-2}$ s$^{-1}$ and $f_{2-10} \sim 4.5\ 10^{-16}$ erg cm$^{-2}$ s$^{-1}$ obtained by Rosati et al. (2002) have been pushed to $f_{0.5-2} \sim 2.4\ 10^{-17}$ erg cm$^{-2}$ s$^{-1}$ and $f_{2-10} \sim 2.1\ 10^{-16}$ erg cm$^{-2}$ s$^{-1}$ by refining the detection techniques (Moretti et al. 2002). The Chandra ACIS-I observations of these fields have been complemented with deep XMM exposures: 180 ks and 370 ks of clean XMM data have been obtained for the CDFN (Miyaji et al. 2002) and the CDFS (Hasinger et al. 2002), respectively. The full source catalogs of the 1 Ms ACIS-I observations of the CDFN and CDFS have been already released (Brandt et al. 2001; Giacconi et al. 2002), while the additional 1 Ms ACIS-I observation of the CDFN and the XMM observations of the CDFN and CDFS are actually under analysis and only preliminary results are available (Alexander et al. 2002; Miyaji et al. 2002; Hasinger et al. 2002). Deep Chandra HRC and XMM exposures are on going in the Lockman Hole (see Hasinger et al. 2001 for the analysis of the first XMM data), where the deepest ROSAT and ASCA surveys were already performed (the ROSAT UDS, Lehmann et al. 2001, and the ASCA Deep Survey, Ishisaki et al. 2001). Other examples of combined Chandra/XMM deep surveys are being carried out in the Lynx field (Stern et al. 2002), in the

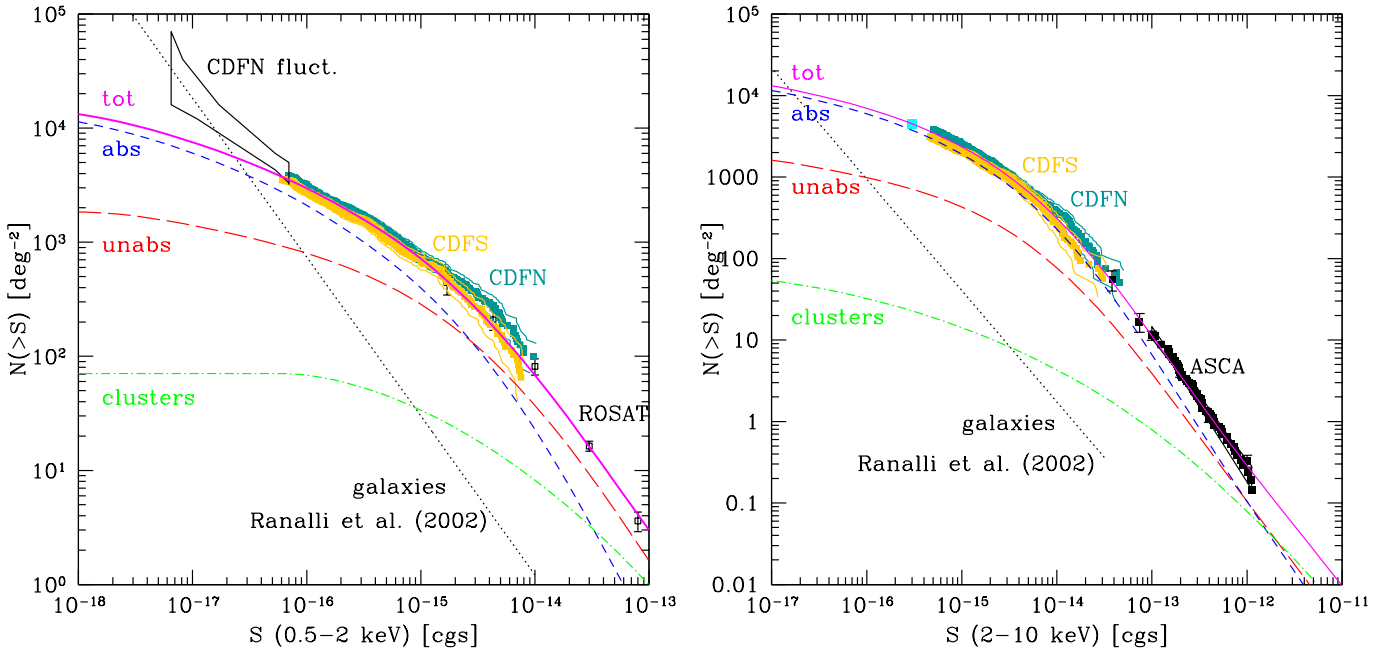


Fig. 2. Soft (*left*) and hard (*right*) logN-logS compared with the predictions of model B by GSH01. Different curves correspond to the contribution of different classes of objects as labeled. The galaxy counts predicted by the Ranalli et al. (2002) model are also plotted as a dotted line. CDFS and CDFN data are from Rosati et al. (2002) and from Brandt et al. (2001). The CDFN fluctuation analysis box is adapted from Miyaji & Griffiths (2002). ROSAT data are from Miyaji et al. (2000). ASCA data (black squares) at $f_{2-10} = 4\,10^{-14}$, $7\,10^{-14}$ and $> 10^{-13}$ erg cm$^{-2}$ s$^{-1}$ are from Ogasaka et al. (1998), Ueda (2001) and Cagnoni et al. (1998), respectively. The deepest datapoint in the hard logN-logS is from Moretti et al. (2002).

| Survey | RA (J2000) | DEC | X-ray data | $f^a_{0.5-2}$ | $f^b_{2-10}$ | $N^c$ | Reference |
|---|---|---|---|---|---|---|---|
| CDFN | 189.200 | 62.231 | 2 Ms Chandra ACIS-I | 0.1 | 0.1 | 503 | 1 |
| | | | 180 ks XMM | 4 | 2 | $\sim 200$ | 2 |
| CDFS | 53.116 | -27.808 | 1 Ms Chandra ACIS-I | 0.5 | 0.4 | 346 | 3,4 |
| | | | 370 ks XMM | | | | 5 |
| Lockman Hole | 163.179 | 57.480 | 300 ks Chandra HRC | | | | |
| | | | 100 ks XMM | 3.1 | 1.4 | $\sim 200$ | 6 |
| Lynx Field | 132.229 | 44.909 | 180 ks Chandra ACIS-I | 1.7 | 1.3 | 153 | 7 |
| | | | 140 ks XMM | | | | |
| Groth Strip | 214.429 | 52.474 | 200 ks Chandra ACIS-I | | | | |
| | | | 80 ks XMM | 6 | 4 | $\sim 150$ | 2 |
| 13hr field | 203.654 | 37.912 | 120 ks Chandra ACIS-I | | | 214 | 8 |
| | | | 130 ks XMM | 5 | $\sim 3$ | 216 | 8 |

Table 1. Summary of the main deep and moderately deep Chandra/XMM surveys.
[a] Limiting flux in the 0.5-2 keV band in units of $10^{-16}$ erg cm$^{-2}$ s$^{-1}$ .
[b] Limiting flux in the 2-10 keV band in units of $10^{-15}$ erg cm$^{-2}$ s$^{-1}$ .
[c] Number of detected sources.
References: 1)Alexander at al. (2002); 2)Miyaji et al. (2002); 3)Giacconi et al. (2002); 4)Rosati et al. (2002); 5)Hasinger et al. (2002); 6)Hasinger et al. (2001); 7)Stern et al. (2002); 8)Page et al. (2002).

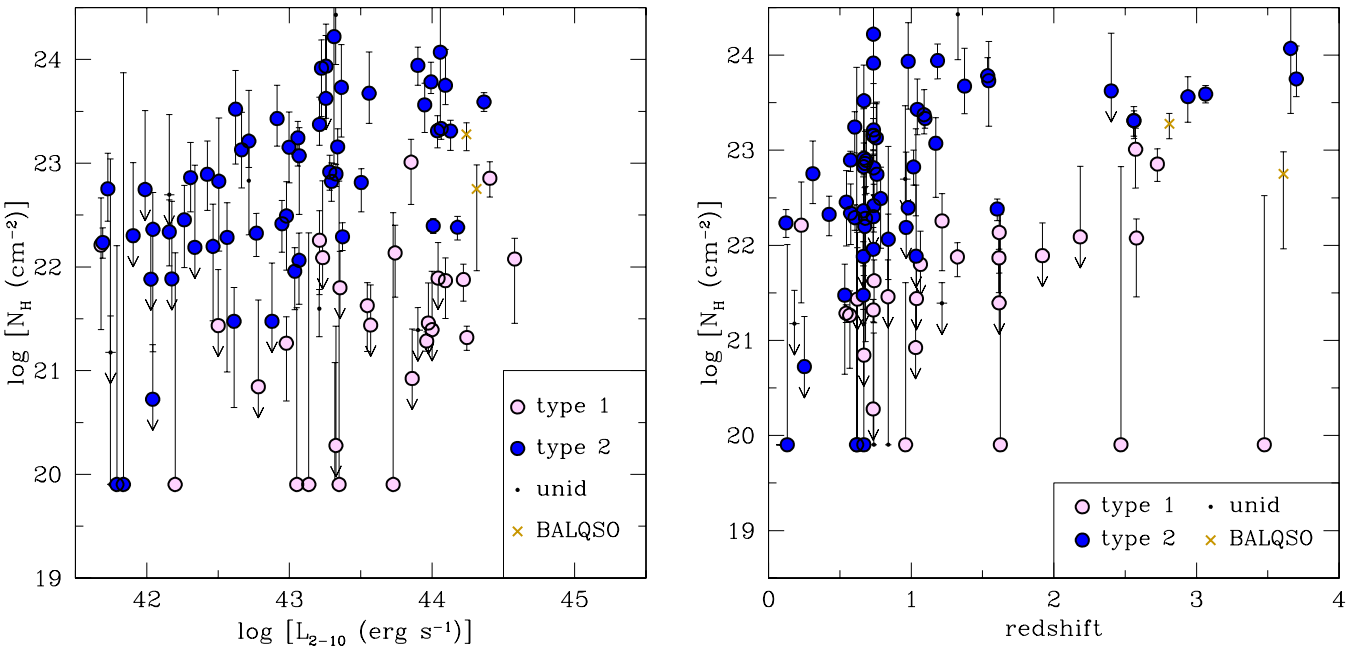


Fig. 3. *Left*: rest-frame absorbing column density versus rest frame, intrinsic (de-absorbed) luminosity in the 2-10 keV band for the CDFS sources with $f_{2-10} > 5\,10^{-16}$ erg cm$^{-2}$ s$^{-1}$ (a cosmological model with $H_0 = 50$ km s$^{-1}$ Mpc$^{-1}$ and $q_0 = 0.5$ has been assumed). Different symbols represent different optical types as labeled. Type 1 AGN do show broad lines, while type 2 AGN do not (see Szokoly et al. in preparation for the detailed classification criteria). Sources with uncertain classification are plotted as dark dots. Obscured QSOs populate the upper-right corner of the plot (with $L_{2-10} > 10^{44}$erg s$^{-1}$ and $N_H > 10^{22}$cm$^{-2}$ ). As already observed in shallower surveys (e.g. HELLAS, Fiore et al. 2001) several broad line AGN are found to have X-ray absorption in excess of $10^{22}$cm$^{-2}$ . *Right*: rest-frame absorbing column density versus redshift for the same source sample. Symbols are the same as in the left panel.

Groth-Westphal strip (Miyaji et al. 2002) and in the 13hr field (Page et al. 2002). A summary of the main deep and moderately deep Chandra/XMM surveys is shown in Table 1.

In the soft band, the deepest observations are detecting sources about two orders of magnitude fainter than those observed by the ROSAT UDS. The progress in the hard X-rays is even higher, since Chandra is now detecting sources $\sim 300$ times fainter than those detected in the ASCA Deep Survey.

As shown by Tozzi et al. (2001a), the integrated emission of all the CDFS sources has already resolved the 2-10 keV background flux measured by HEAO-1. Furthermore, the stacked spectrum of the whole CDFS sample is well described by a powerlaw with $\Gamma = 1.4$ (Tozzi et al. 2001a), in excellent agreement with the measurements of the XRB spectral slope in that energy range (see Fig. 1).

The soft and hard logN-logS calculated in the CDFS and CDFN are confirming the predictions by AGN synthesis models. As shown in Fig 2, the logN-logS curve for model B of GSH01, which is the summed contribution of absorbed AGN, unabsorbed AGN and clusters of galaxies, can reproduce the CDFN and CDFS data at all fluxes. Some deviations are observed in the soft logN-logS when considering the data from the CDFN fluctuation analysis (Miyaji and Griffiths 2002), which are higher than the model expectations. However, as shown in Fig 2 (left), at those faint fluxes a population of normal/starburst galaxies is expected to provide a major contribution (Ptak et al. 2001; Ranalli, Comastri & Setti 2002).

**The sources populating the Deep Surveys**

Due to the extremely faint X-ray fluxes sampled by the deep surveys, for standard X-ray to optical flux ratios, 8-10 meter class telescopes are needed for the optical followup (see Hornschemeier 2002 for a review). Optical spectra of the X-ray sources in the CDFN are being obtained at Keck (Barger et al. 2002), while

the VLT is primarily exploited for optical spectroscopy of CDFS sources (Szokoly et al. in preparation; see also Hasinger et al. 2002). The spectroscopic completeness in the CDFS and CDFN is roughly $40-50\%$, but it increases up to $\sim 80\%$ when considering the inner part of the fields and sources with X-ray fluxes well above the survey sensitivity limit. A direct redshift estimate is not possible for a significant fraction of X-ray sources even with 10m class telescopes: $\sim 25\%$ of the X-ray sources have counterparts fainter than R=25, while $\sim 15\%$ do not have any counterpart down to R magnitudes of 26.1-26.7 (Giacconi et al. 2002). Nevertheless, photometric redshifts are being determined for optically faint sources. The counterparts of the X-ray sources reveal a broad variety of optical properties. Broad line and narrow line AGN are commonly found, but there are also sources with no obvious high-excitation emission lines in their spectra. When the optical classification is uncertain, the X-ray properties such as the X-ray luminosity and hardness ratio, in addition to the X-ray to optical flux ratio ($f_x/f_{opt}$), can be used to discriminate between nuclear and stellar activity (see e.g. Hasinger et al. 2002). As shown by Hornschemeier et al. (2002) and Giacconi et al. (2002), about $15-20\%$ of the sources populating the deep X-ray surveys have $f_x/f_{opt}$ values typical of normal/starbursts galaxies, with this fraction being higher in the soft band and towards faint fluxes. On the contrary, the contribution of non-active galaxies is negligible when selecting sources with 2-10 keV fluxes above a few $10^{-15}$ erg cm$^{-2}$ s$^{-1}$ .

In Fig. 3 (left panel) the absorbing column of CDFS sources, measured from the X-ray spectral fit, is plotted against their rest frame, intrinsic (i.e. de-absorbed) X-ray luminosity in the 2-10 keV band ($L_{2-10}$), calculated assuming $H_0 = 50$ km s$^{-1}$ Mpc$^{-1}$ and $q_0 = 0.5$. When the photon statistics is low, the spectral index is fixed to $\Gamma = 1.8$ and the absorbing column measured accordingly. Different symbols correspond to different optical types (only sources with $f_{2-10} > 5\,10^{-16}$ erg cm$^{-2}$ s$^{-1}$ and good spectroscopic redshift are shown). A fraction of AGN with broad optical lines are found to have X-ray absorption in excess of $10^{22}$cm$^{-2}$ , confirming the optical to X-ray classification mismatch already observed in shallower X-ray surveys (e.g. HELLAS, Fiore et al. 2001; Comastri et al. 2001). A number of sources are found to have $L_{2-10} > 10^{44}$erg s$^{-1}$ and $N_H > 10^{22}$cm$^{-2}$ , which can be well considered the faint tail of the QSO2 population (a similar result has been found in the Lockman Hole by Mainieri et al. 2002a). Given the relatively low space density of luminous sources, the high-luminosity tail of the QSO2 population is best sampled by shallow, wide area surveys.

**The source redshift distribution**

Most of the sources identified in the CDFN, CDFS and Lockman Hole are found to be at $z < 1$ (see Fig. 10 of Barger et al. 2002 for the CDFN; Fig. 9 of Tozzi et al. 2001b for the CDFS; Fig. 1 of Mainieri et al. 2002b for the Lockman Hole). Synthesis models of the X-ray background predict that at these faint fluxes the X-ray source redshift distribution is peaked at $z \sim 1.3-1.5$, in contrast with the observed data. A direct comparison between the published distributions and the model predictions is however complicated by the following effects:

1) optical identifications are still far from complete. In general, the still unidentified sources are expected to be at higher redshift than those already observed.

2) $\sim 15-20\%$ of the sources populating the deep surveys are non-active galaxies at $z < 1$.

3) given the narrow field of view of the deep surveys (0.1-0.2 deg$^2$) the redshift distribution could be dominated by the presence of large scale structures. This is indeed the case in the CDFS (Gilli et al. 2003), where narrow spikes in the source redshift distribution have been found at $z = 0.67$ and $z = 0.73$, and also in the CDFN, where redshift structures have been found at $z = 0.84$ and $z = 1.02$ (Barger et al. 2002).

Nevertheless, the spectroscopic completeness can be significantly increased by selecting sources with an X-ray flux well above the survey limit in those subregions with higher optical coverage. Also, if only bright and hard X-ray selected sources are considered, the percentage of non-AGN objects drops dramatically.

In Fig. 4 (left) it is shown the redshift distribution of the 93 sources with $f_{2-10} > 5\,10^{-15}$ erg cm$^{-2}$ s$^{-1}$ in the central regions of the CDFS, CDFN, Lockman Hole (Mainieri et al. 2002a), Lynx field (Stern et al. 2002) and SSA13 field (Mushotzky et al. 2000). The spectroscopic completeness of this combined sample is $\sim 80\%$. Sources belonging to the large scale structures observed in the CDFS and CDFN have been excluded. The redshift distribution predicted by model B of GSH01 at the same limiting flux and normalized to 116 objects ($93/116 = 80\%$) is also shown in Fig. 4 (left). An excess of sources at $z < 1$ with

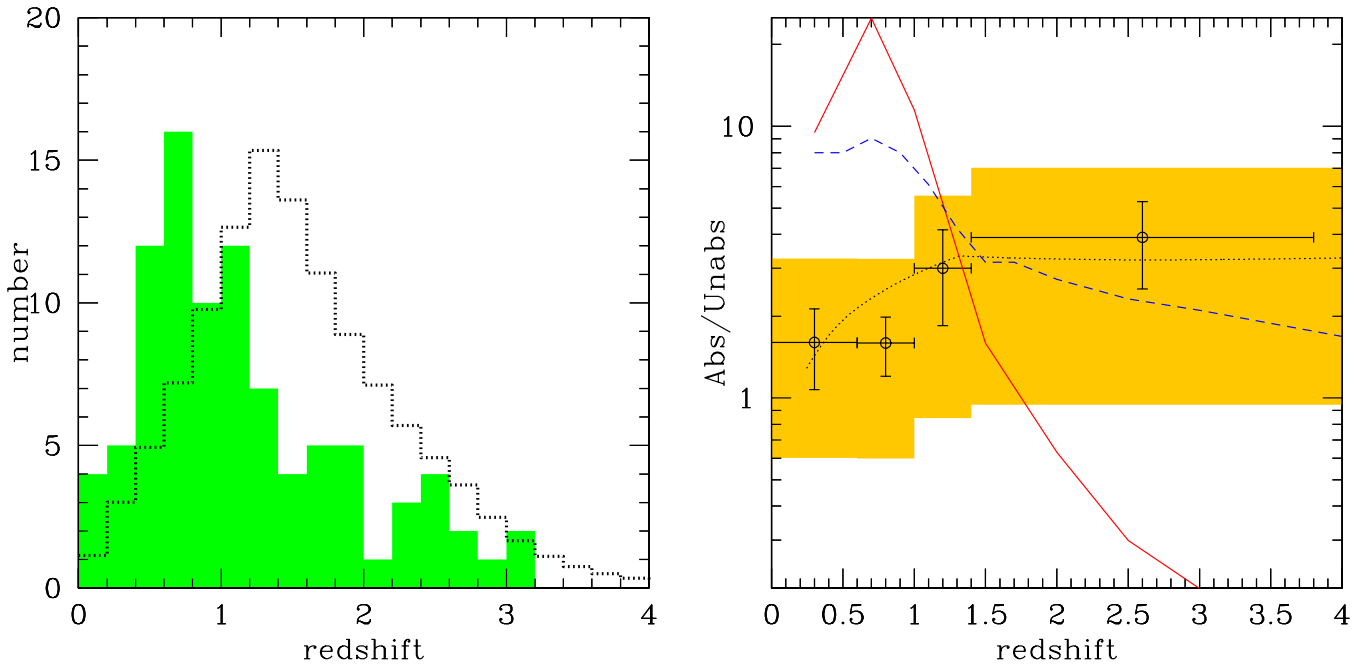


Fig. 4. *Left*: Redshift distribution for the 93 X-ray sources with $f_{2-10} > 5\,10^{-15}$ erg cm$^{-2}$ s$^{-1}$ in the central regions of the CDFS, CDFN, Lockman Hole, Lynx field, and SSA13 field (see text; only spectroscopic redshifts are considered). With this selection the achieved spectroscopic completeness is $\sim 80\%$. Sources belonging to large scale structures in the CDFS and CDFN are excluded. The data (shaded area) are compared with the predictions of model B by GSH01 at the same limiting flux (dotted line), normalized to 116 sources (93/116 = 80%). A clear excess of sources is observed at $z < 1$ with respect to the model predictions.
*Right*: Ratio between AGN with log$N_H > 22$ and log$N_H < 22$ as a function of redshift for the sources with $f_{2-10} > 5\,10^{-16}$ erg cm$^{-2}$ s$^{-1}$ detected in the inner regions of the CDFS and CDFN (the spectroscopic completeness of this sample is $\sim 60\%$). Redshift bins have been chosen to contain approximately the same number of sources. The predictions for the Franceschini et al. (2002) model and the Gandhi & Fabian (2002) model at comparable fluxes ($f_{2-10} = 8\,10^{-16}$ and $5\,10^{-16}$ erg cm$^{-2}$ s$^{-1}$ , respectively) are also plotted as a solid and dashed line, respectively. The shaded area shows the possible range covered by the data under the two extreme assumptions that the unidentified sources (40% of the sample) are either all obscured or all unobscured (see text). Both models seem to predict too many obscured AGN at $z < 1$. For comparison the prediction by model B of GSH01 at $f_{2-10} > 5\,10^{-16}$ erg cm$^{-2}$ s$^{-1}$ is plotted as a dotted line.

respect to the model predictions is still found in this clean sample.

## DO OBSCURED AGN EVOLVE LIKE STARBURST GALAXIES?

A solution to this discrepancy has been recently proposed by Franceschini, Braito & Fadda (2002), who suggested that obscured AGN undergo a very fast evolution up to $z = 0.8$. The physical scenario supporting this idea is that obscured AGN are related to the fast evolving starburst population necessary to reproduce the ISO mid-infrared counts (Franceschini et al. 2001). By shifting most of the obscured AGN at $z < 1$, that model nicely reproduces the redshift distribution observed in the deep surveys; unobscured sources are however still needed to explain the high redshift tail of the distribution (see Fig. 5 in Franceschini et al. 2002). A more refined model has been recently worked out by Gandhi & Fabian (2002), who also make a connection between obscured AGN with the infrared starburst population. Even this model is able to reproduce the low-z peak in the redshift distribution, with the main contribution at $z < 1$ provided by obscured AGN. Both these new models are bound to predict a decrease with redshift in the ratio between obscured and unobscured AGN, which can be checked on the CDFN and CDFS data. In Fig. 4 (right) it is shown the ratio between the number of sources with log$N_H > 22$ and log$N_H < 22$ in the CDFS and CDFN

as a function of redshift. Only sources with $f_{2-10} > 5\,10^{-16}$ erg cm$^{-2}$ s$^{-1}$ and in the inner regions of the two fields have been considered[1], to get a spectroscopic completeness of $\sim 60\%$. The combined sample contains 194 sources with measured redshift, 85 from the CDFS and 109 from the CDFN. As in Fig. 2, the absorption column density for the CDFS sources has been calculated by fitting the X-ray spectra with a simple absorbed power-law, fixing the slope to $\Gamma = 1.8$ when the photon statistics is low. About 64% of the considered CDFS sources have absorption in excess of $10^{22}$cm$^{-2}$ . The absorption column density for the CDFN sources has been taken from Fig. 18 of Barger et al. (2002), who derived the $N_H$ values from the source hardness ratios (fixing the photon index to $\Gamma = 1.8$). While the redshifts considered in the CDFS subsample are all spectroscopic, one third of the redshifts in the CDFN subsample are photometric. Similarly to what found in the CDFS, 72% of the considered CDFN sources have $N_H > 10^{22}$cm$^{-2}$ . The shaded area in Fig. 4 (right) shows the possible range covered by the ratio between the number of sources with column density above and below $10^{22}$cm$^{-2}$ under the two extreme assumptions that the unidentified sources are either all obscured or all unobscured. Although the incompleteness is likely to increase with redshift, it is assumed to be 40% in each redshift bin. The ratio predicted by the Franceschini et al. (2002) model, calculated at a comparable limiting flux is also shown as a solid line. At low redshifts the predicted ratio highly overestimates the data, while the opposite is true at high redshifts. It is noted that the Franceschini et al. model is a simple approximation, since only one class of obscured sources is considered (with $N_H \sim 2\,10^{23}$cm$^{-2}$ ). In the more refined model by Gandhi & Fabian (2002), where several classes of sources with different obscuration are assumed, the discrepancy is less significant, but still the ratio between AGN with $\log N_H > 22$ and $\log N_H < 22$ is overestimated at $z < 1$.

Fig. 4 (right) indicates that at $z < 1$ the ratio between AGN with $\log N_H > 22$ and $\log N_H < 22$ is lower than $\sim 3$, suggesting that the low-z peak in the redshift distribution is not due exclusively to obscured sources. Since the XLF of unobscured AGN is not properly sampled by ROSAT at low luminosities and moderate redshifts ($10^{42}$erg s$^{-1}$ at $z \sim 1$), a regime now accessible to Chandra, the assumed extrapolations might not be correct (preliminary results suggest this is indeed the case; see Cowie et al. 2003 and Hasinger et al. 2003) and a new determination of the AGN XLF is therefore needed.

## CONCLUSIONS

The deep surveys have finally established that the cosmic X-ray background in the 2-10 keV band is produced by the integrated emission of obscured and unobscured AGN, confirming to the first order the main prediction of population synthesis models. Now it is possible to put tighter constraints to the model parameter space and study in detail the AGN evolution down to luminosities of $10^{42}$erg s$^{-1}$ at $z \sim 1$, checking if previous assumptions were correct. The AGN redshift distribution observed in the deep surveys seems to peak at $z < 1$, while standard synthesis models were expecting a peak at $z = 1.3 - 1.5$. Assuming that obscured AGN evolve very quickly up to $z < 1$ does solve the discrepancy in the redshift distribution but predicts too many obscured AGN among low-z sources. A new determination of the XLF of unobscured AGN in the regime not covered by previous shallower surveys is therefore needed, which has then to be implemented into the XRB synthesis models.

## ACKNOWLEDGMENTS

I gratefully acknowledge all the members of the Chandra Deep Field South collaboration.

## REFERENCES

Akiyama, M. et al., Optical Identification of the ASCA Large Sky Survey, *Astrophys. J.*, **532**, 700-727, 2000.

Alexander, D.M. et al., Resolving the Source Populations that Contribute to the X-ray Background: The 2 Ms Chandra Deep Field-North Survey, *Astron. Nach.*, in press, 2002 [astro-ph/0210308].

Barger, A.J. et al., X-Ray, Optical, and Infrared Imaging and Spectral Properties of the 1 Ms Chandra Deep Field North Sources, *Astron. J.*, **124**, 1839-1885, 2002.

Brandt, N.W. et al., The Chandra Deep Field North Survey. V. 1 Ms Source Catalogs, *Astron. J.*, **122**, 2810-2832, 2001.

Cagnoni, I. et al., A Medium Survey of the Hard X-Ray Sky with the ASCA Gas Imaging Spectrometer:

[1]About 1/4 of the CDFN sample is actually selected at fluxes above $5\,10^{-15}$ erg cm$^{-2}$ s$^{-1}$ (see Barger et al. 2002).

The (2–10 keV) Number Counts Relationship, *Astrophys. J.*, **493**, 54-61, 1998.

Comastri, A. et al., The contribution of AGNs to the X-ray background, *Astron. & Astrophys.*, **296**, 1-12, 1995.

Comastri, A. et al., The BeppoSAX High Energy Large Area Survey (HELLAS) - III. Testing synthesis models for the X-ray background, *Mon. Not. Roy. Ast. Soc.*, **327**, 781-787, 2001.

Cowie, L. et al., The Redshift Evolution of the 2-8 keV X-Ray Luminosity Function, *Astrophys. J.*, **584**, L57-60, 2003.

Fabian, A.C. et al., Do nuclear starbursts obscure the X-ray background?, *Mon. Not. Roy. Ast. Soc.*, **297**, L11-15, 1998.

Fiore, F. et al., The BeppoSAX High Energy Large Area Survey (HELLAS) - II. Number counts and X-ray spectral properties, *Mon. Not. Roy. Ast. Soc.*, **327**, 771-780, 2001.

Franceschini, A. et al., A long-wavelength view on galaxy evolution from deep surveys by the Infrared Space Observatory, *Astron. & Astrophys.*, **378**, 1-29, 2001.

Franceschini, A., V. Braito, and D. Fadda, Origin of the X-ray background and AGN unification: new perspectives, *Mon. Not. Roy. Ast. Soc.*, **335**, L51-L56, 2002.

Gendreau, K.C. et al., ASCA Observations of the Spectrum of the X-Ray Background, *Pub. Ast. Soc. Jap.*, **47**, L5-L9, 1995.

Georgantopoulos, I. et al., A deep ROSAT survey - V. The extragalactic populations at faint fluxes, *Mon. Not. Roy. Ast. Soc.*, **280**, 276-284, 1996.

Gandhi, P., and A.C. Fabian, X-ray background synthesis: the infrared connection, *Mon. Not. Roy. Ast. Soc.*, in press, 2002 [astro-ph/0211129].

Giacconi, R. et al., Chandra Deep Field South: The 1 Ms Catalog, *Astrophys. J. Suppl.*, **139**, 369-410, 2002.

Gilli, R., G. Risaliti, and M. Salvati, Beyond the standard model for the cosmic X-ray background, *Astron. & Astrophys.*, **347**, 424-433, 1999.

Gilli, R., M. Salvati, and G. Hasinger, Testing current synthesis models of the X-ray background, *Astron. & Astrophys.*, **366**, 407-417, 2001.

Gilli, R. et al., Tracing the large scale structure in the CDFS, *Astrophys. J.*, submitted, 2003.

Gruber, D.E., The Hard X-Ray Background, in The X-ray background, eds. X. Barcons and A.C. Fabian, pp. 44-53, Cambridge Univ. Press, Cambridge, 1992.

Gruber, D.E. et al., The Spectrum of Diffuse Cosmic Hard X-Rays Measured with HEAO 1, *Astrophys. J.*, **520**, 124-129, 1999.

Hasinger, G. et al., XMM-Newton observation of the Lockman Hole. I. The X-ray data, *Astron. & Astrophys.*, **365**, L45-L50, 2001.

Hasinger, G. et al., Understanding the sources of the X-ray background: VLT identifications in the Chandra/XMM-Newton Deep Field South, *The Messenger*, **108**, 11-16, 2002.

Hasinger, G. et al., Formation and Evolution of Supermassive Black Holes in Galactic Centers: Observational Constraints in The Emergence of Cosmic Structure, eds. S.S. Holt and C. Reynolds, 2003 [astro-ph/0302574].

Hornschemeier, A.E. et al., The Weak Outnumbering the Mighty: Normal Galaxies in Deep Chandra Surveys, *Astron. Nach.*, in press, 2002 [astro-ph/0211487].

Hornschemeier, A.E., The Challenge to Large Optical Telescopes from X-ray Astronomy, in Science with 6-10 m Class Telescopes, proc. SPIE, in press, 2002 [astro-ph/0210044].

Ishisaki, Y. et al., ASCA Deep Survey in the Lockman Hole Field, *Pub. Ast. Soc. Jap.*, **53**, 445-457, 2001.

Kinzer, R.L. et al., Diffuse Cosmic Gamma Radiation Measured by HEAO 1, *Astrophys. J.*, **475**, 361-372, 1997.

Kushino, A. et al., Study of the X-Ray Background Spectrum and Its Large-Scale Fluctuation with ASCA, *Pub. Ast. Soc. Jap.*, **54**, 327-352, 2002.

Lehmann, I. et al., The ROSAT Deep Survey. VI. X-ray sources and Optical identifications of the Ultra Deep Survey, *Astron. & Astrophys.*, **371**, 833-857, 2001.

Lumb, D.H. et al., X-ray background measurements with XMM-Newton EPIC, *Astron. & Astrophys.*, **389**, 93-105, 2002.

Madau, P., G. Ghisellini, and A.C. Fabian, The Unified Seyfert Scheme and the Origin of the Cosmic X-Ray Background, *Mon. Not. Roy. Ast. Soc.*, **267**, L17-L21, 1994.

Mainieri, V. et al., XMM-Newton observation of the Lockman Hole. II. Spectral analysis, *Astron. & Astrophys.*, **393**, 425-438, 2002a.

Mainieri, V. et al., XMM-Newton observations of the Lockman Hole : Spectral analysis, in New Visions of the X-ray Universe in the XMM-Newton and Chandra Era, eds. F. Jansen et al. 2002b [astro-ph/0202211].

Maiolino, R., and G.H. Rieke, Low-Luminosity and Obscured Seyfert Nuclei in Nearby Galaxies, *Astrophys. J.*, **454**, 95-105, 1995.

Marshall, F.E. et al., The diffuse X-ray background spectrum from 3 to 50 keV, *Astrophys. J.*, **235**, 4-10, 1980.

Miyaji, T., G. Hasinger, and M. Schmidt, Soft X-ray AGN luminosity function from it ROSAT surveys. I. Cosmological evolution and contribution to the soft X-ray background, *Astron. & Astrophys.*, **353**, 25-40, 2000.

Miyaji, T. et al., XMM-Newton View of the Hubble Deep Field-North and Groth-Westphal Strip Regions, *Astron. Nach.*, in press, 2002 [astro-ph/0211343].

Miyaji, T., and R.E. Griffiths, Faint-Source Counts from Off-Source Fluctuation Analysis on Chandra Observations of the Hubble Deep Field-North, *Astrophys. J.*, **564**, L5-L8, 2002.

Moretti, A. et al., The Brera Multiscale Wavelet Detection Algorithm Applied to the Chandra Deep Field-South: Deeper and Deeper, *Astrophys. J.*, **570**, 502-513, 2002.

Mushotzky, R.F. et al., Resolving the extragalactic hard X-ray background, *Nature*, **404**, 459-464, 2000.

Ogasaka, Y. et al., Sky surveys with ASCA — Deep Sky Survey, *Astron. Nach.*, **319**, 43-46, 1998.

Page, M.J. et al., X-ray and optical properties of X-ray sources in the 13hr XMM-Newton/Chandra deep survey, *Astron. Nach.*, in press, 2002 [astro-ph/0212035].

Pompilio, F., F. La Franca, and G. Matt, The X-ray background and the evolution of AGN, *Astron. & Astrophys.*, **353**, 440-446, 2000.

Ptak, A. et al., The Consequences of the Cosmic Star Formation Rate: X-Ray Number Counts, *Astrophys. J.*, **559**, L91-L95, 2001.

Ranalli, P., A. Comastri, and G. Setti, The 2-10 keV luminosity as a Star Formation Rate indicator, *Astron. & Astrophys.*, in press, 2002.

Risaliti, G., R. Maiolino, and M. Salvati, The Distribution of Absorbing Column Densities among Seyfert 2 Galaxies, *Astrophys. J.*, **522**, 157-164, 1999.

Rosati, P. et al., The Chandra Deep Field-South: The 1 Million Second Exposure, *Astrophys. J.*, **566**, 667-674, 2002.

Setti, G., and L. Woltjer, Active Galactic Nuclei and the spectrum of the X-ray background, *Astron. & Astrophys.*, **224**, L21-L23, 1989.

Stern, D.E. et al., SPICES II: Optical and Near-Infrared Identifications of Faint X-Ray Sources from Deep Chandra Observations of Lynx, *Astron. J.*, **123**, 2223-2245, 2002.

Tozzi, P. et al., Resolving the X-ray background with Chandra: the 1 MS observation of the Chandra Deep Field South, in Clusters of Galaxies and the High Redshift Universe Observed in X-rays, eds. D. Neumann, F. Durret and J. Tran Thanh Van, 2001a.

Tozzi, P. et al., New Results from the X-Ray and Optical Survey of the Chandra Deep Field-South: The 300 Kilosecond Exposure. II, *Astrophys. J.*, **562**, 42-51, 2001b.

Ueda, Y., Results from X-ray Surveys with ASCA, in X-ray astronomy : stellar endpoints, AGN, and the diffuse X-ray background, eds. N.E. White, G. Malaguti and G.G.C. Palumbo, pp. 396-405, 2001.

Vecchi, A. et al., The BeppoSAX 1-8 keV cosmic background spectrum *Astron. & Astrophys.*, **349**, L73-L76, 1999.

Wilman, R.J., and A.C. Fabian, Fitting the spectrum of the X-ray background: the effects of high-metallicity absorption, *Mon. Not. Roy. Ast. Soc.*, **309**, 862-870, 1999.

Warwick, R.S., and T.P. Roberts, The extragalactic X-ray background at 0.25 keV, *Astron. Nach.*, **319**, 59-62, 1998.

Wright, E.L. et al., Interpretation of the COBE FIRAS CMBR spectrum, *Astrophys. J.*, **420**, 450-456, 1994.